PROF. PLACID RODRIGUEZ AWARD LECTURE

Wire Arc Additive Manufacturing by Cold Metal Transferred (CMT) Arc Welding Process

Dr. S. Malarvizhi
Professor, Center for Materials Joining and Research (CEMAJOR),
Department of Manufacturing Engineering, Annamalai University, Annamalai Nagar - 608002.
Email: jeejoo@rediffmail.com

DOI : 10.22486/iwj.v53i1.191278

ABSTRACT

Additive manufacturing (also known as 3D printing) is considered as a disruptive technology to produce limited number of high value components with topologically optimized complex geometries and functionalities that is not achievable by traditional manufacturing. Wire Arc Additive Manufacturing (WAAM) allows to produce metal components by depositing filler wire layer by layer with the help of welding arc. WAAM is a potential future process to manufacture complex parts without much of tooling required or with less material wastage. Cold Metal Transfer (CMT) arc welding technique offers high stable arc with less heat input and high welding speed which results in less distortion. The aim of this work is to optimize the critical welding parameters in CMT arc welding in order to achieve a stable arc to develop the component and to analyse the mechanical and micro structure properties fabricated using ER308L wire. In this experimental work, welding parameters in CMT process were optimized for the stainless steel component deposited using ER308L filler wire. From this investigation it was found that the weld speed, current, stick out and voltage were the most influencing parameters to achieve stable arc and for process feasibility. After the completion of fabrication, the component was tested non-destructively in order to confirm the soundness of the weld deposits and to ensure the component is free from porosity and lack of fusion between the layers. The component was sectioned and specimens were extracted from vertically at three sections (Top, middle and bottom). Mechanical properties were evaluated as per the ASTM standards. Microstructural analysis was done using optical microscopy and scanning electron microscopy. It is found that the mechanical properties and microstructural characteristics are uniform throughout the height of the component.

Keywords: Wire Arc additive manufacturing; gas metal arc welding; stainless steel; cold metal transfer; mechanical properties; microstructure.

1.0 INTRODUCTION

Additive manufacturing is a promising technology to reduce cost and time for making the components by reducing wastage and number of processes involved in advanced manufacturing. Wire arc additive manufacturing is one of the advanced manufacturing technologies which finds numerous applications in aerospace, defense, and railways and in oil and gas industry. Lot of research is taken up in wire arc additive manufacturing using different process methods such as laser welding, gas tungsten arc welding and gas metal arc welding. As outlined by Filippo et al. [1] Additive Manufacturing processes represents one of the most relevant innovative method in manufacturing sector for the production of metal components and it provides number of benefits in making complex geometry parts. Cold metal transfer (CMT) arc welding is an excellent process for the application of wire arc additive manufacturing (WAAM) because of its stable arc, wire movement integrated in process controls, controlled heat input and extremely low spatter. Layer by layer welding is achieved in CMT process since it has highly controlled arc movement and thus the process has been selected. As described by Gerhard Posch et al. [2] in his work CMT is based on a high-frequency forward and backward movement of the welding wire electrode and it offers an almost spatter-free and absolute precise, periodic detachment of accurately defined droplets from the filler wire at very low process energies. A robotic CMT system can deposit minimum thicknesses in the range of 2 - 4 mm in wire arc additive manufacturing process. Stainless steels essential property is their resistance to corrosion, especially in saline solutions, under oxidizing conditions. This is the result of a thin adhesive film of Cr_2O_3, which forms on the surface at room temperature and which is self-healing when scratched or otherwise damaged. Among the different types of stainless steel available, austenite stainless steel is the most commonly used for industrial applications because of its properties of easy formability, weldability and service at elevated temperature. ER308L was used for the metal deposition in this work since it has been used extensively for several applications.

2.0 EXPERIMENTAL WORK

2.1 WAAM System

A 6 axis industrial robot connected with TPS4000CMT power source was used as the WAAM system for this process. Remote control processing unit helps to control the parameters for the process. The robot controller pendant was used to teach the programming and to coordinate the robot motions and welding process. CMT liquid coolant torch was connected to the robot arm for welding of continuous deposition of weld layers. The working table alignment was checked and adjusted using level indicator. Process parameters had been optimized using the Remote control unit. Filler wire used for the material deposition was ER308L. Synergic line for the filler wire was incorporated in the power source. The **Fig. 1** shows the system setup of WAAM and welding of WAAM model.

2.2 Parameter Optimization

The process parameters were optimized using trial and error method in order to achieve stable arc to deposit weld layer one above others. High amperage causes high heat input and made the material to melt while depositing one layer over another. Weld speed and wire feed speed also impacts the weld bead shape. Less speed increases the heat input and forms wide weld bead. High speed results in improper merging between layers. The CMT system was synergic based control system, thus change in current also changes the voltage and wire feed speed. Higher stick out deflects the arcing to large extent and produces spatter while building more number of layers. The optimized parameters for the WAAM model were shown in the below **Table 1**.

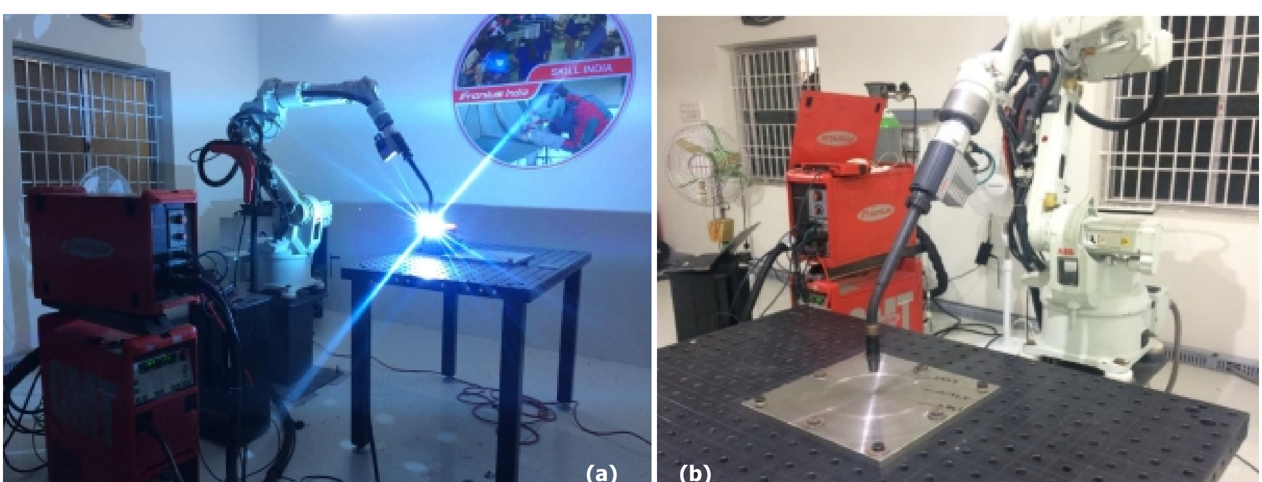

Fig. 1 : (a) WAAM setup; (b) Component welding

Table 1 : Parameters used for WAAM

Parameter	Values	Parameter	Values
Current	205 A	Burnback correction	0.00 s
Voltage	13 V	Power offset	2.0 m/min
Wire feed speed	7.0 m/min	Mode	S2 step
Weld speed	25 cm/min	Starting current	100 %
Stick out	12-16 mm	Slope	0.1 s
Arc length correction	-9%	Final current	30 %
Dynamic correction	5.0	Start time	0.3 s
Gas pre flow	0.8 s	End time	0.6 s
Gas post flow	0.9 s	Slope 2	0.4 s

2.3 Robot Teaching and Welding

A circle path program was programmed into the robot control pendant to weld a cylinder shaped component. Markings were done at 45° spacing over a 360° path to teach the tracing path as shown in **Fig. 2(a)**. Robot arm had been moved to each points to teach the path coordinates and saved to trace the circle path during welding. Weaving of 12 mm has been given in order to achieve the component thickness and a vertical shift of 2.1 mm given for each layer.

First layer welding was done with slower speed compared to the following above layers. The first layer need to melt the substrate material and thus slow welding speed was maintained. The **Fig. 2(b)** shows the red hot condition of the component due to the continuous welding.

2.4 Inspection and Machining

The **Fig. 3 (a)** shows the finished welded component after cooling. The component was cleaned and non-destructive testing was done to ensure the model is free from porosity and lack of fusion between the multiple layers welding. After the completion of Radiographic testing and dye penetrant testing, the model was machined by lathe turning to remove the excess weld material on both sides. The pipe kept for the base was cut and removed during machining before proceeding to tensile testing and micro structure analysis. The **Fig. 3 (b)** shows the component after machining and **Fig. 6** shows the sectioned pieces for analysis at different levels. The **Fig. 3 (c)** represents the 3D model of the component which shows how the specimens were extracted from the machined component. Wire cut EDM process has been used to cut the samples from the component.

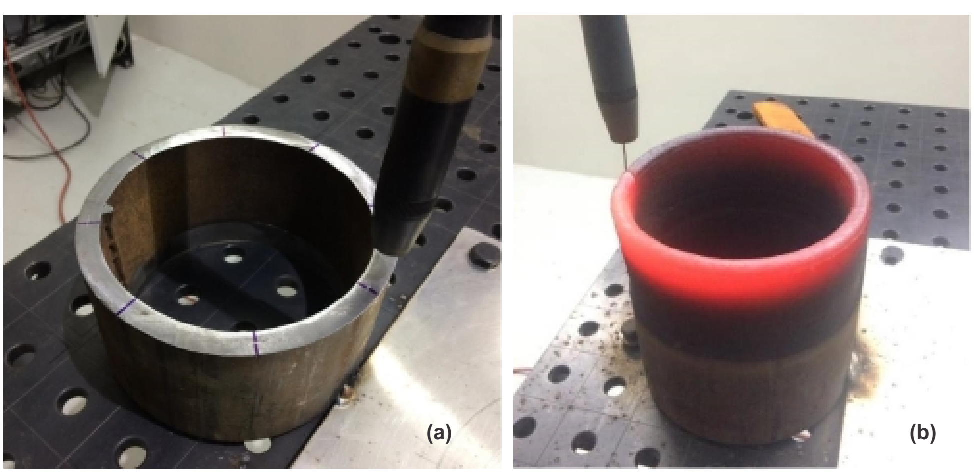

Fig. 2 : (a) Robot Teaching; (b) During WAAM Process

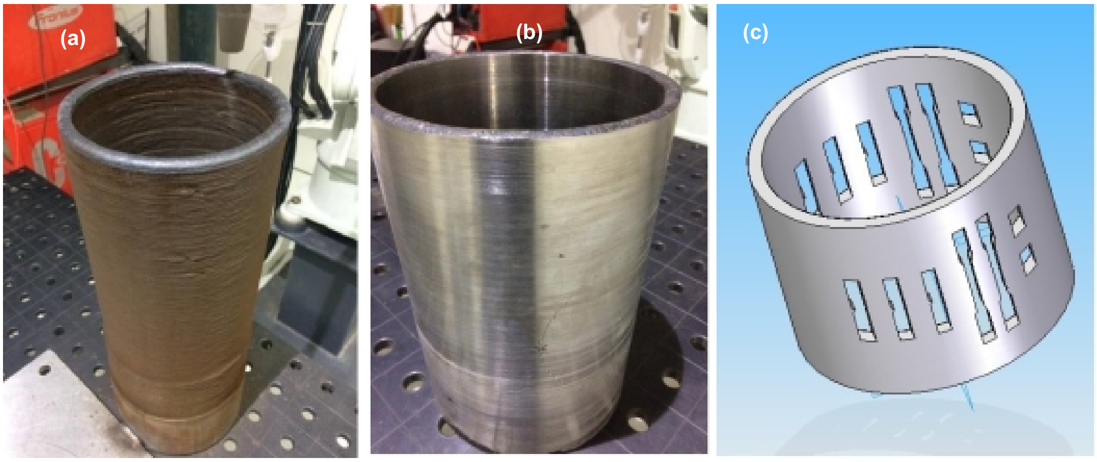

Fig. 3 : (a) As deposited component; (b) Machined component; (c) Specimen extraction

Table 2 : Chemical Composition

	C	Cr	Ni	Mo	Mn	Si	P	S	Cu
Filler	0.01	19.59	9.59	0.10	1.88	0.47	0.024	0.001	0.13
Top	0.019	19.65	9.53	0.11	1.83	0.46	0.027	0.003	0.13
Middle	0.019	19.62	9.55	0.11	1.82	0.47	0.027	0.004	0.13
Bottom	0.019	19.59	9.66	0.11	1.80	0.45	0.027	0.003	0.13

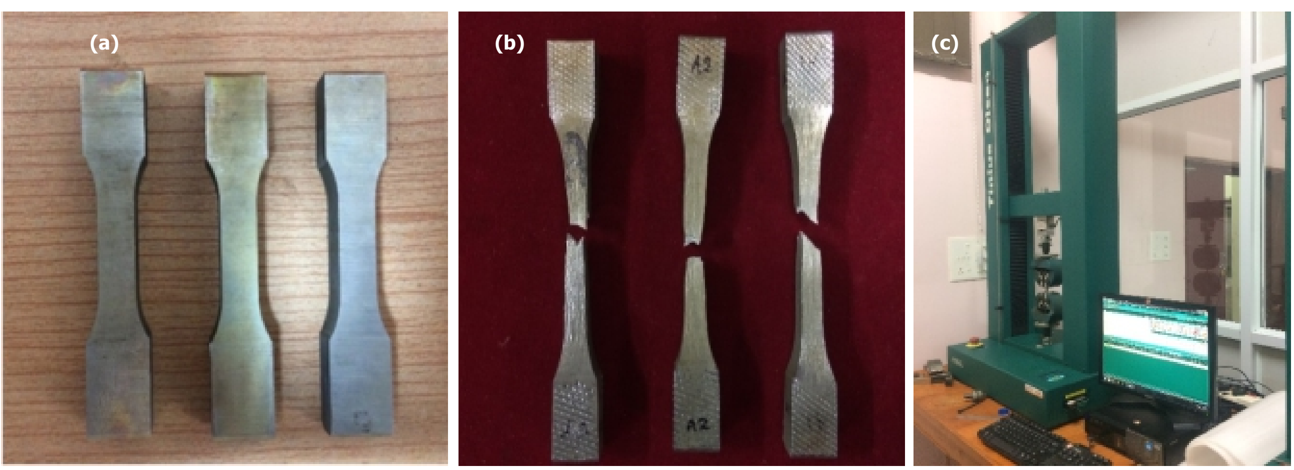

Fig. 4 : (a) Before testing; (b) After testing; (c) UTM

3.0 RESULTS

3.1 Chemical Analysis

The chemical composition of the filler wire and the weld metal are presented in **Table 2**. Samples were extracted from all the three sections and spectroscopy test conducted in Spectro Analytical GMBH make optical emission spectrometer and the software used is Spectral Analyser Vision MX. The spectroscopy results show that chemical composition is even in all the three samples and it matches with the filler metal chemical composition.

3.2 Tensile Properties

The component was divided into three sections as top (100 mm from top), middle and bottom (100 mm from bottom) to analyze the micro structure at different regions and to investigate the mechanical properties. Specimens were extracted from the component vertically by using Wire cut EDM

Table 3 : Tensile Properties

Specimen ID	Sample Location	UTS (MPa)	% of Elongation (GL 25 mm)	NTS (MPa)	NSR Ratio
1A	Top	571	76	676	1.18
1B	Top	568	72	678	1.19
1C	Top	569	72	672	1.18
2A	Middle	598	64	700	1.17
2B	Middle	574	62	716	1.25
2C	Middle	582	68	708	1.22
3A	Bottom	574	60	667	1.16
3B	Bottom	575	68	672	1.17
3C	Bottom	570	66	675	1.18

process. Three reduced section tensile samples and three notch tensile samples have been extracted from each section. Specimens were prepared as per ASTM Sub size specimen standards of gage length 25 mm and tested in 50KN load capacity Tinius Olsen H50KL tensile testing machine which is shown in **Fig. 4(c)**. Specimens taken from top section before testing and after testing were shown in **Figs. 4(a)** and **4(b)**.

Table 4 : Vickers Hardness

Hardness Values (HV)		
Location	**Weld Bead**	**Inter- Layer**
Top	169, 180, 172	180, 179, 168
Middle	181, 187, 172	186, 193, 175
Bottom	169, 181, 174	168, 167, 168

The tensile test results are shown in **Table 3**. The results shows that the tensile values range from 568 MPa to 598 MPa. The tensile values show almost uniform strength throughout the component with better elongation properties as well. There is no much difference observed in the tensile strength of the specimens extracted from different sections. The change in tensile values are only ±5% which can be seen from the obtained values in the below **Table 3**. The obtained tensile strength and elongation are also well above the minimum requirement of ER308L wire 520 MPa and 35% as defined by the code ASME Sec II Part C. The notch tensile values and the calculated NSR values are also presented in **Table 3**. The NSR values are above 1 which proves that the fabricated component is notch ductile in nature.

The hardness was measured at all three sections from the component top, middle and bottom at both the weld bead location and at weld bead interface locations and the results are presented in **Table 4**. Measurements were carried out at 0.5 kg load with 15 seconds loading time using Vickers hardness tester. The results show that the hardness values are uniform, acceptable and they exhibit the similar hardness values of normal welded ASS.

3.4 Charpy Impact Toughness

Charpy specimens were extracted vertically from similar locations at top, middle and bottom. Testing carried out at -196°C to analyse the impact properties for sub-zero applications. The results are presented in **Table 5**. The obtained impact values shows very good impact properties even at sub-zero temperatures.

3.5 Macro and Microstructure Analysis

The macro specimens were extracted from all the three regions of the weld component, etched and the macro photographs

Table 5 : Impact Toughness at -196°C

Location	Weld Bead	Inter- Layer
Top	74, 64, 68	1.30, 1.17, 1.34
Middle	66, 86, 76	1.31, 1.68, 1.35
Bottom	74, 78, 74	1.21, 1.26, 1.42

taken are shown in the below **Fig. 5**. Etchant were prepared by adding 5 gm of copper chloride in 30 ml of HNO_3. The different weld layers are clearly visible in the macro photographs and the photographs show the weld beads are free from defects and the layers are properly merged. The macro photographs shows that the weld is free from cracks and other visual defects.

The specimens were extracted from all the three cut sections to analyze microstructure. The specimens were polished, etched and analyzed in optical microscope. Micro structure was analyzed at both the weld bead area and the interface area between adjacent layers.

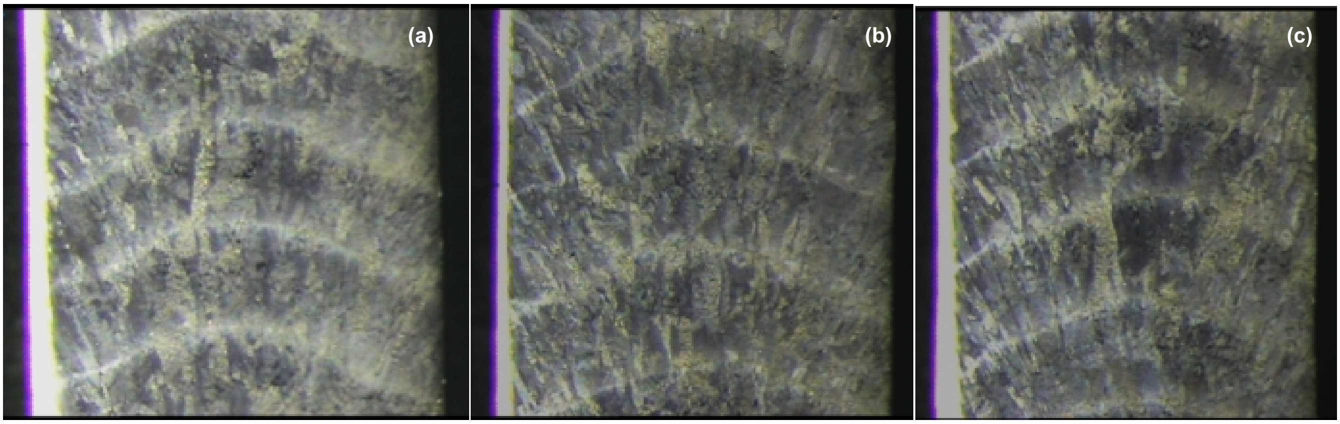

Fig. 5 : Macro photographs (a) Top; (b) Middle; (c) Bottom

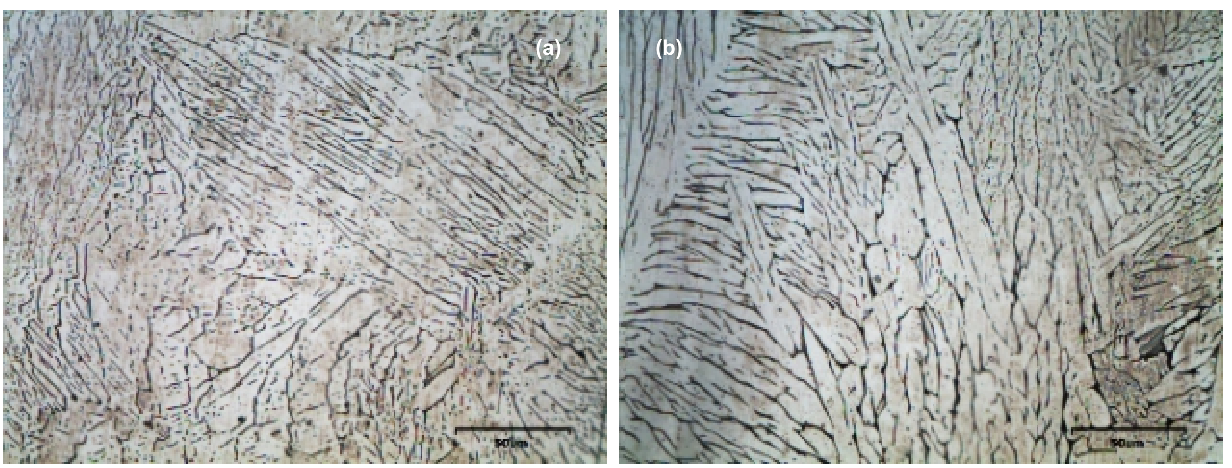

Fig. 6 : Microstructure from top region (a) Weld; (b) Inter-layer

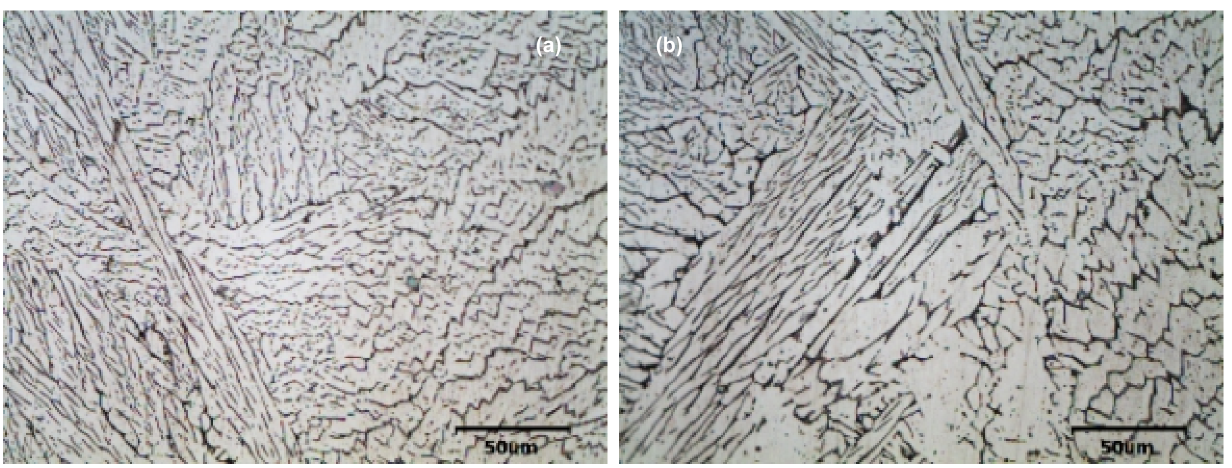

Fig. 7 : Microstructure from middle region (a) Weld; (b) Inter-layer

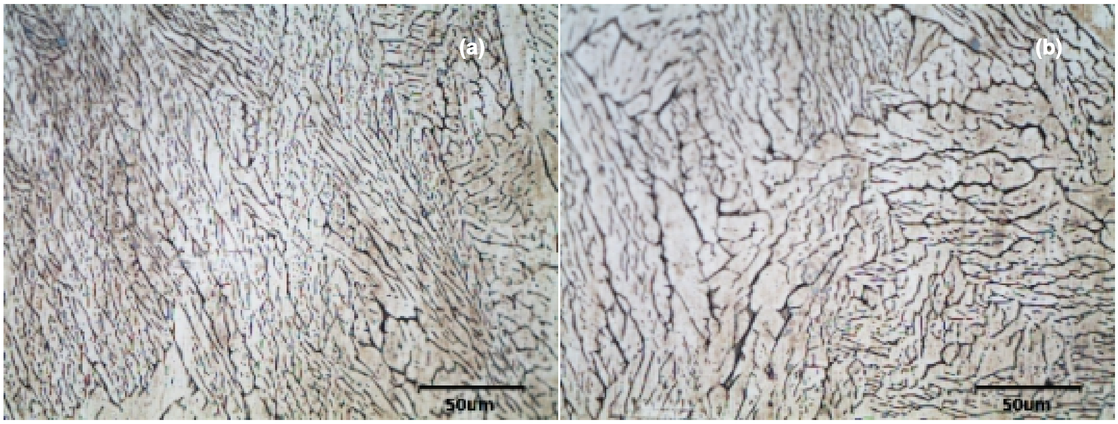

Fig. 8 : Microstructure of bottom region (a) Weld; (b) Inter-layer

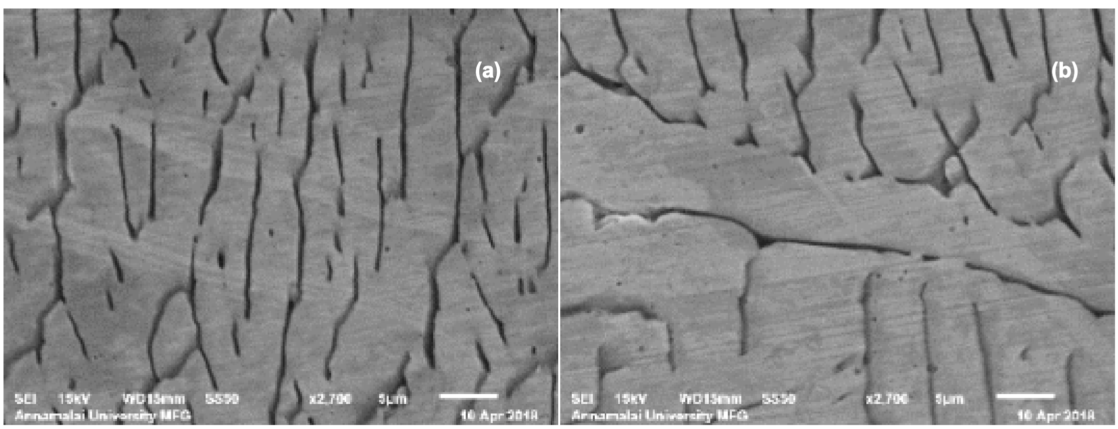

Fig. 9 : SEM Microstructure

The above **Figs. 6-8** show the microstructure of weld bead and bead interface taken at 200x and 400x magnifications from top, middle and bottom regions respectively. The black line shows the presence of delta ferrite and the remaining light colored areas are austenite. The micro structure is almost even and uniform in all the three sections. There is no significant change in the microstructure at different sections because of the continuous weld in WAAM process. The microstructure reveals the microstructure of WAAM components are similar to that of conventional weld joints. The **Fig. 9** shows the clear microstructure of austenitic matrix and the second image shows the inter-layer between the weld beads.

3.6 Fractograph

The fractography of the broken tensile specimens were analyzed and shown in **Fig. 10**. The **Fig. 10 (a)** shows the macro image of the prepared specimen. The **Fig. 10 (b), (c)** and **(d)** shows the fractured surface in higher magnifications and it shows the micro voids initiated at second-phase particles and it exhibits dimpled ruptures of elliptical shapes which clearly denotes ductile fracture.

4.0 DISCUSSION

WAAM component of cylindrical model welded in CMT process and mechanical and micro structure analysis has been done. The investigation shows that current, voltage, weld speed and stick out were determined to be the influencing parameters for the WAAM process. Programming and parameter optimization were done for the cylinder model. The tensile properties were studied at different locations and found similar throughout the component. The obtained values are much higher than the standard minimum value 520 MPa for the filler wire and the elongation also ranges from 60 to 75%. The NSR values prove that the component fabricated is ductile in nature.

Superior impact properties were obtained in the charpy test which was tested at temperature well below the zero level at -

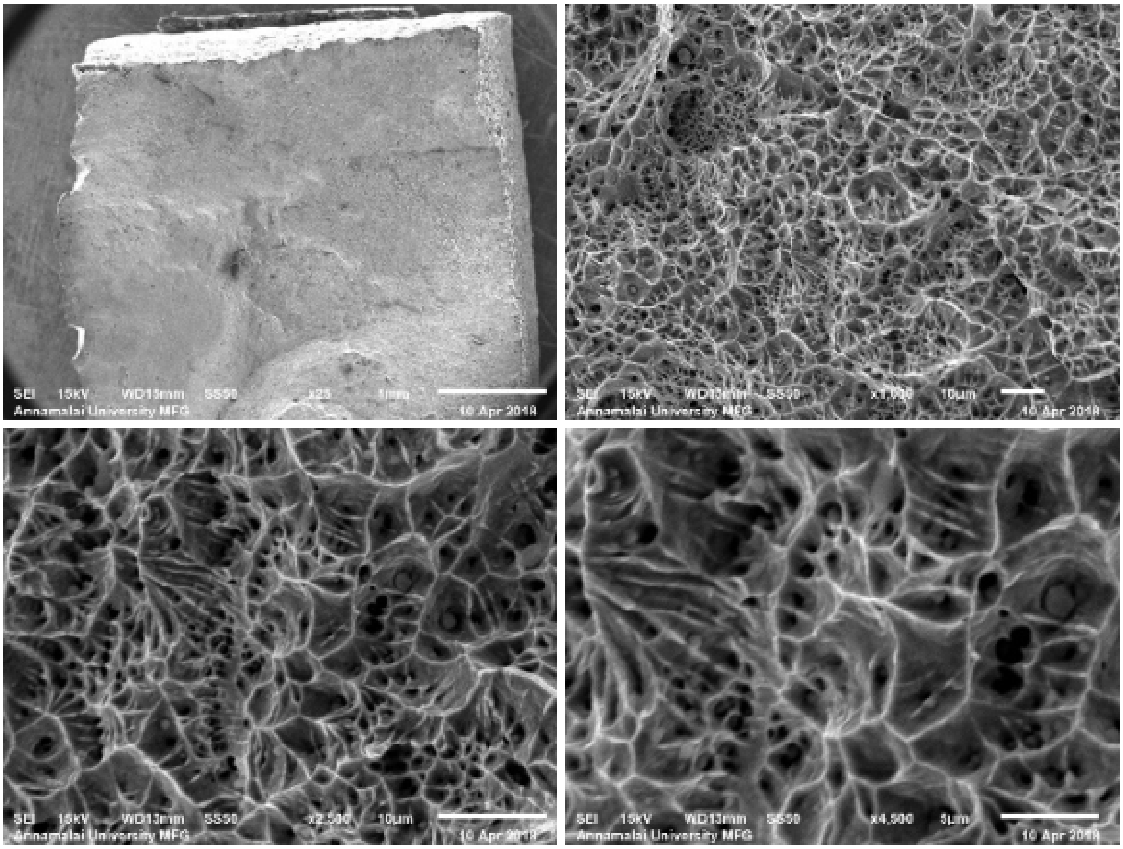

Fig. 10 : SEM- fractograph images

196°C. Austenite and delta ferrite structures were seen throughout the component. There was no significant change in microstructure and mechanical properties at different locations analyzed and the SEM fractograph image shows the dimpled ruptures and micro voids present in the fracture surface. Thus the result shows that WAAM as a potential process for developing critical components instead of subtractive machining processes.

5.0 CONCLUSIONS

From this investigation the following conclusions are derived,

1. CMT - WAAM can be a potential process for manufacturing components. It reduces the wastage of materials, tool design and machining time and thus it provides economical solution and less lead time for component development.
2. Future scope includes development of fixtures and programs to design and fabricate critical design components in WAAM system.
3. Analysis of mechanical properties and microstructure characterization on different materials such as Inconel and Titanium can be done for aerospace, automotive, oil and gas, medical and other applications.

ACKNOWLEDGEMENT

The author wishes to record sincere thanks to Dr. V. Balasubramanian, Professor and Director, Centre for Materials Joining and Research (CEMAJOR) Annamalai University for all the technical and non-technical support to do this investigation. The author would like to thank Mr. Sam Stephen Raj (M.E (Welding Engineering) student) and Mr. Addanki Ramaswamy (Ph.D scholar) for their help and support to carryout this investigation. The author also would like to thank M/s. Fronius (India) Private Limited, Chennai for providing WAAM facility to carry out this investigation and Mr. Suman, Fronius India Pvt. Ltd. for his contribution in this work.

REFERENCES

[1] Montevecchia F, Venturinia G, Scippaa A and Campatellia G (2016); Finite element modelling of WAAM process, CIRP. 55 pp.109-114.

[2] Posch G, Chladil K and Chladil H (2017); Material properties of CMT-Metal additive manufactured duplex stainless steel blade-like geometries, International Institute of Welding.

[3] Ding D, Shen C and Pan Z, Robotic wire and arc additive manufacturing: Innovative fabrication of large metal components, Australasian Welding Journal – Volume 60.

[4] Shi X, Ma S, Liu C, Wu Q, Lu J, Liu Y and Shi W (2017); Selective laser melting-wire arc additive manufacturing hybrid fabrication of Ti-6Al-4V alloy: Microstructure and mechanical properties, Materials Science & Engineering A. 684, pp.196–204.

[5] Williams SW, Martina F, Addison AC, Ding J, Pardal G and Colegrove P (2015); Wire + Arc Additive Manufacturing, Institute of metals, minerals and mining.

[6] Mehnen J, Ding J, Lockett H and Kazanas P (2010); Design for Wire and Arc Additive Layer Manufacture, CIRP Design conference.

[7] Ugla AA and Yilmaz O, Deposition – Path generation of SS308 components manufactured by TIG welding- based Metal deposition process, Springer.

[8] Abe T and Sasahara H, Dissimilar metal deposition with a stainless steel and nickel -based alloy using wire and arc-based AM, Precision Engineering.

[9] Antonysamy AA, Microstructure, Texture and Mechanical Property Evolution during Additive Manufacturing of Ti6Al4V Alloy for Aerospace Applications, University of Manchestar, Doctorate Thesis.

[10] Busachi A, Erkoyuncu J, Colegrove P, Martina F and Ding J (2015); Designing a WAAM Based Manufacturing System for Defence Applications, Elsevier CIRPe.